



# Numerical finite element investigation of thin steel shear walls retrofitted with CFRP layers under reversed cyclic loading

Mehdi Ebadi-Jamkhaneh<sup>1</sup> · Denise-Penelope N. Kontoni<sup>2,3</sup>

Received: 18 April 2022 / Revised: 18 May 2022 / Accepted: 20 May 2022 / Published online: 15 June 2022  
© The Author(s), under exclusive licence to Springer Nature Switzerland AG 2022

## Abstract

The lateral stiffness and shear strength of the steel plate shear wall (SPSW) system are provided by the diagonal tension field generated in the infill plate. The SPSW is a relatively new structural system, which has been accepted by several regulations and codes. A new form of this system is the composite steel plate shear wall (CSPSW), which consists of a steel plate and fiber-reinforced polymer (FRP) layers at one or both sides of the infill plate. The advantages of this system are low weight, high energy absorption, and low space occupancy. In this paper, the retrofitting method using carbon fiber-reinforced polymer (CFRP) sheets on one and both sides of the steel infill plate is used. Several parameters, including infill plate thickness, number of surface coverage of CFRP sheet, and fiber orientation, are considered in determining the behavior of the system under cyclic loading. Nonlinear static analysis is used in the ABAQUS finite element (FE) program for 16 numerical models. After ensuring the proper performance of the simulated model with the reference test specimen, numerical models were developed. The results of numerical FE studies showed that using CFRP sheets compared to non-retrofitted models can increase the yield strength and lateral load-bearing capacity of the system. In some cases, energy absorption increased by 50%. Besides, adding more layers of CFRP sheets did not have much effect on lateral load-bearing capacity, whereas it was able to convert the failure mode from the diagonal buckling of the wall to CFRP layer rupture and, in some cases, to the separation of the CFRP sheet.

**Keywords** Steel plate shear wall (SPSW) · Carbon fiber-reinforced polymer (CFRP) · CFRP layer · Reversed cyclic loading · Energy absorption · Hysteresis curve

## 1 Introduction

Steel plate shear wall (SPSW) plays an important role in improving the seismic behavior of structures. In a thin SPSW that has a high slenderness ratio, the shear buckling of the infill plate usually dominates the system. A SPSW is made of a steel plate surrounded by horizontal and vertical

boundary elements. This system acts like a girder beam, in which the columns are its flanges, the floor beams are its stiffeners, and the steel infill plate is as its web [1]. In this system, unlike a plate girder, in which the flanges do not play a significant role in absorbing forces due to the weakness of the flanges, in steel shear walls, due to the strength of the columns, the columns can play a good role in load-bearing [2, 3].

Numerous numerical and experimental studies have been performed to date on SPSWs and have shown that the SPSW system has good ductility, stiffness, and lateral load resistance using buckling behavior. The effect of pinching in hysteresis loops under cyclic loads due to steel infill plate may reduce the energy absorption capacity of SPSWs. Several researchers have suggested the use of plates with low-yield stress to improve the performance of SPSW [4, 5]. In this case, a large buckling resistance is created by forming a tensile field. The formation of a tensile field after the shear buckling of a thin infill plate can help the SPSW system

✉ Denise-Penelope N. Kontoni  
kontoni@uop.gr; kontoni.denise@ac.eap.gr

Mehdi Ebadi-Jamkhaneh  
m.ebadi@du.ac.ir

<sup>1</sup> Department of Civil Engineering, School of Engineering, Damghan University, Damghan, Iran

<sup>2</sup> Department of Civil Engineering, School of Engineering, University of the Peloponnese, 26334 Patras, Greece

<sup>3</sup> School of Science and Technology, Hellenic Open University, 26335 Patras, Greece

to maintain resistance against the horizontal force. On the other hand, the tensile forces generated by the tensile field are transmitted directly to the vertical boundary element (VBE), and this can cause its premature failure [6]. Elastic shear buckling of steel plate usually reduces the stiffness and strength of the SPSW system. In addition, the periodic formation of incline tensile field and compressive field under cyclic load causes damage to the infill plate, which has been proven by numerical testing and modeling [7, 8].

Many modern SPSWs use stiffeners to prevent out-of-plane buckling. The design of thin-walled SPSWs was first proposed in the 1980s by Thorburn et al. at the University of Alberta, based on the results of studies on plate girders [9]. They focused on theoretical and test studies only on thin-sheet SPSWs and, while conducting experiments to calculate their ultimate load-bearing capacity, they replaced the thin web plate with a series of diagonal tensile rods. Studies by researchers [9, 10], which have been performed on steel shear panels with sheets of different thicknesses and stiffeners with different dimensions and arrangements, have shown that the panels with stiffeners on both sides had better behavior than panels with stiffeners on one side. Studies on the strengthening of SPSWs by Alinia and Dastfan [11], Alinia and Shirazi [12], and Habashi and Alinia [13] revealed that the buckling of these sheets could be delayed by using additional stiffeners, but the manufacturing cost will increase. The main disadvantage of this technique is the excessive use of steel materials. At the same time, the failure of the steel plate in this technique usually occurs after the overall yielding of the steel frame, which, therefore, cannot act as a means of energy dissipation device. Another proposed method to enhance the seismic behavior of the SPSW was changing the shape of the infill plate like a corrugation in the plate [14–16].

Other researchers [17–19] investigated the use of thin steel plates with buckling-resistant plywood. The steel plate can reach its full plastic strength before shear buckling. The results of their studies also showed that by adding a concrete coating to the steel plate, the in-plane stiffness increases, and its buckling behavior is improved. The concrete layer also distributes better stress in the steel plate and expands the tensile field lines over a wide region. However, buckling-resistant plywood made of concrete increases the weight of the shear wall, and due to the low tensile strength of the concrete, this plywood may crack under sudden loads such as earthquakes. Several investigations on improving the seismic performance of thin SPSW were performed by a strategy of using openings and slits in the infill wall [20, 21]. They used different shapes of openings and slits in their studies to determine the seismic performance of thin SPSW by FE analysis. The results indicated that the shape and location of the openings had a considerable effect on the performance of SPSW. Zhang et al. [22] suggested a

new type of double-steel-plate shear wall. Based on their results, the mechanical properties and failure rules of the wall were revealed, and the failure mechanism of the wall was obtained. Li et al. [23] numerically investigated the seismic behavior of a novel buckling-restrained steel plate shear wall. The new shear wall was an excellent steel plate shear wall to be used in high-rise structures to resist horizontal loadings.

Another method for reinforcing SPSWs is the use of CFRP layers, which has been considered by various researchers in recent decades. Hatami et al. [24] investigated the nonlinear behavior of SPSWs and steel shear walls with CFRP. Laboratory studies were performed to evaluate the effects of volume, fiber angle, and panel length on the seismic behavior of these walls. Experimental results showed that polymer fibers increase the energy absorption, stiffness, and load-bearing capacity of SPSWs but reduce their ductility. Nateghi-Alahi and Khazaei-Poul [25] experimentally studied the nonlinear behavior of composite shear walls strengthened with glass fiber-reinforced polymer (GFRP). Experiments were performed to evaluate the effect of the number of GFRP layers and the position of layers on stiffness, shear strength, dissipative energy, and other main seismic parameters on composite steel shear walls. The results showed that the ultimate shear strength and energy dissipation can be significantly increased by GFRP. Dan [26] conducted a study to investigate the possibility of using fibers' polymer to reinforce concrete composite shear walls under seismic loading. Seddighi et al. [27] numerically studied the behavior of retrofitted SPSW with different patterns of FRP laminates. The results revealed that the full coverage of the SPSW has the maximum effectiveness of reinforcement. Also, they found a reduction in the ductility index due to the delay in the commencement of failure in the steel infill wall.

In this study, the behavior of thin SPSW under cyclic loading is investigated numerically in the ABAQUS finite element (FE) program by considering parameters such as infill plate thickness, number of CFRP layers, and arrangement of CFRP sheets. The results are discussed in the form of force–displacement hysteresis, energy absorption capacity, and ductility curves. The main aim of this study is to determine the seismic performance of the rehabilitated system.

## 2 Numerical modeling

To analyze each model in the ABAQUS software [28], the material properties of the elements must be known. Typically, these properties include the mechanical and thermal properties of the material. On the other hand, the properties of the materials introduced in the software can be isotropic or orthotropic. In the models of this paper, the properties

of all materials are assumed to be isotropic [29, 30]. The materials and their properties are introduced to the software. In this study, for St37 steel, the modulus of elasticity is assumed to be 206 GPa, and its shear modulus is assumed to be 79.23 GPa.

CFRPs have been used to strengthen the steel shear wall. The modulus of elasticity, Poisson's ratio, thickness, tensile strength, and ultimate strain of CFRP are 240 GPa, 0.3, 0.176 mm, 3800 MPa, and 1.5%, respectively. In all beam-to-column connections in ABAQUS software, the C3D8R element is used to mesh the model. An automatic meshing algorithm is used in all models, because the automatic meshing of ABAQUS software is very powerful and often produces proper elements (in terms of placement, fineness of the element in sensitive areas, etc.). After determining the elements of the model, loading should be applied to the model, which includes determining the type of analysis, boundary conditions, and applying loads. Due to the fact that in each of the models, loads are applied to the model statically at each stage, the type of analysis is also introduced as static to the program. The modified Newton–Raphson method is used for nonlinear analysis [31]. In addition, the top and bottom of the column are assumed to be fixed, and these support boundary conditions should be applied to the model. Then, the program asks the user to introduce the nodes of the model that should be constrained. In the models of this research, instead of selecting all the nodes at the end of the column, by defining a rigid plane at the base of the columns, only one point of the rigid plate is fixed, and by selecting the ENCASTRE option, all degrees of freedom of this node are restricted (Fig. 1). The displacement control type of loading is applied in all FE models. The concentrated load is imposed on the rigid plate at the bottom of the

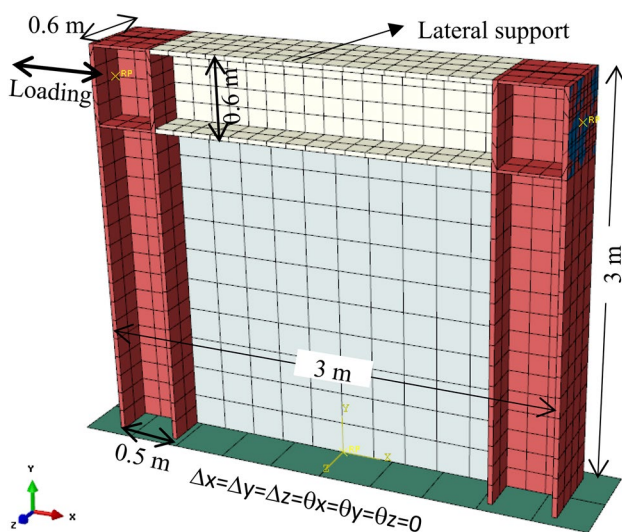


Fig. 1 Support conditions for the end of the column

column to use the force resulting from the displacement in the support position to draw the force–displacement curve. The loading history is shown in Fig. 2.

### 3 Numerical modeling validation

Hatami et al. [24] experimentally tested two samples of SSW and CSSW. The members of the beam and the column of the frame are made of double IPE200 beam of ST37 type steel with two plates with a thickness of 12 mm and 3 mm connected to the flange of the members. The width and height of the tested specimen are 2 m and 1 m, respectively. Also, cyclic load with a frequency of 0.017, 1, 2, and 3 Hz is entered into the system. The thickness and density of the CFRP sheet are 0.176 mm and 0.03 N/m<sup>3</sup>, respectively. After modeling and extracting the two force–displacement curves, the CSSW test sample and the FE model were compared with each other in Fig. 3. Accordingly, the maximum load-bearing capacity of a numerical model was 565.5 kN, which was a difference of 2.8% compared to the test sample (582.0 kN). Also, the amount of absorbed energy in the numerical model under cyclic loads is 15.2 kJ, which is 2.5% more than the laboratory specimen.

### 4 Introducing simulated models

In the present work, 16 models are used, as described in Table 1. In Table 1, the abbreviations are as follows: MRF means a moment frame with medium ductility, and SSW means the steel shear wall. The number after that is the thickness of the steel wall, the letter C indicates the use of CFRP sheet, and the number after the letter C indicates whether the CFRP sheet is one-sided or two-sided. The letter

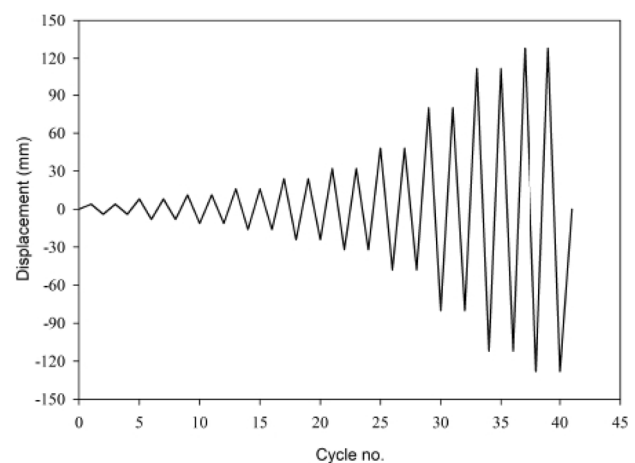
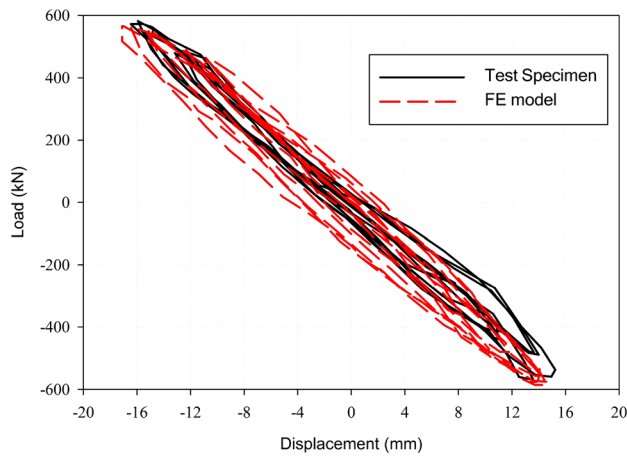


Fig. 2 Reversed cyclic loading history



**Fig. 3** Comparison of force–displacement diagram of the CSSW test sample and the FE model

**Table 1** The 16 numerical models

Model name	Steel plate thickness (mm)	Polymer sheet placement arrangement	Side of polymer sheet placement
MRF	–	–	–
SSW3	3	–	–
SSW3C1F	3	Total coverage	One-sided
SSW3C1X	3	× coverage	One-sided
SSW3C2F	3	Total coverage	Two-sided
SSW3C2X	3	× coverage	Two-sided
SSW5	5	–	–
SSW5C1F	5	Total coverage	One-sided
SSW5C1X	5	× coverage	One-sided
SSW5C2F	5	Total coverage	Two-sided
SSW5C2X	5	× coverage	Two-sided
SSW7	7	–	–
SSW7C1F	7	Total coverage	One-sided
SSW7C1X	7	× coverage	One-sided
SSW7C2F	7	Total coverage	Two-sided
SSW7C2X	7	× coverage	Two-sided

F or X at the end means a complete cover or cross coverage. Also, the width and height of the floor in all FE model is equal to 3 m. Beam and column sections were also considered according to the reference sample.

## 5 Results

All numerical models are subjected to reversed cyclic loading, and the results are presented and evaluated in the form of force–displacement hysteresis curves and the distribution of plastic areas in different parts of the system.

### 5.1 Steel wall with a thickness of 3 mm

Figure 4 shows the force–displacement hysteresis curve of the MRF model. The maximum shear capacity in this model is 430 kN. The maximum base shear of the flexural frame is 430 kN, and the displacement is about 118 mm. The initial stiffness of the steel moment frame is approximately equal to 17.5 kN/mm, the displacement ductility index of the model is equal to 6.34, and the energy absorption is approximately 95 kJ. The failure mechanism in this model is that first the beam in the two areas at the beginning and near the joint undergoes local buckling flange, and the plastic joint is formed in the fourth cycle, which causes a slight reduction in load-bearing capacity. This confirms the design philosophy of “weak beam—strong column”.

In Fig. 5, the hysteresis curve is shown for a set of numerical samples made with a 3 mm steel infill plate with and without FRP sheets. By adding only one steel infill plate between the frame elements with a thickness of 3 mm, the load-bearing capacity of the frame has increased from 430 to 3500 kN. In fact, it has increased by 630%. Also, the ductility coefficient in the case of using an infill plate with a thickness of 3 mm is equal to 9.14. This indicates an increase in shear capacity, energy dissipation, and an increase in the ductility of the system. The amount of energy dissipation is equal to 300 kJ, which is approximately 2.16 times the value of absorbed energy compared to the MRF model.

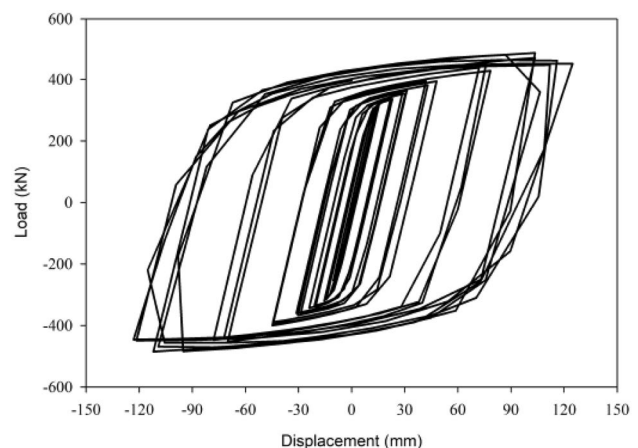


**Fig. 4** Force–displacement diagram of the MRF model



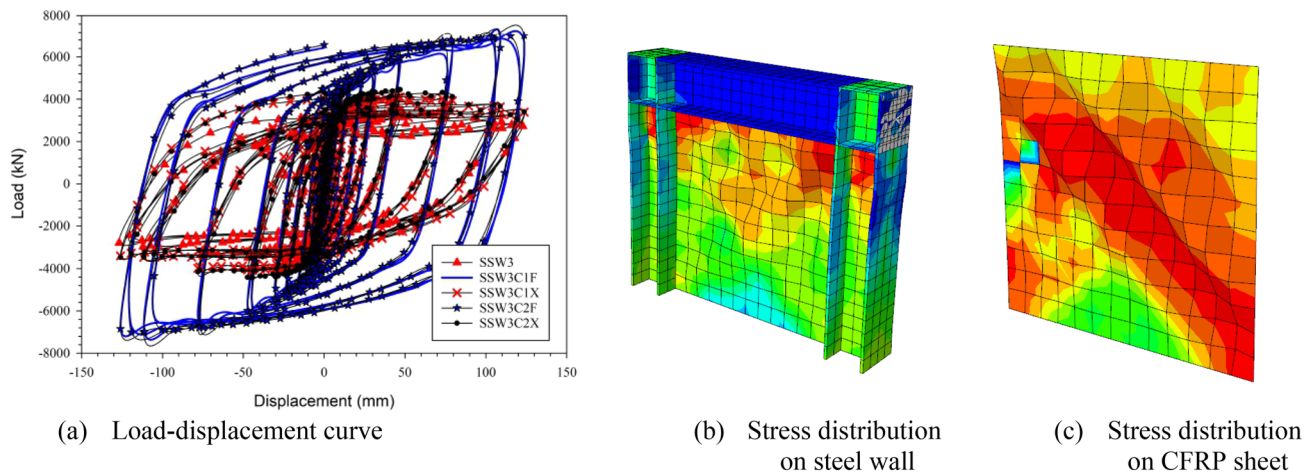


**Fig. 5** Comparison of force–displacement diagram of the frame with 3 mm thick SPSW

By adding only one layer of CFRP with a thickness of 0.176 mm, the load-bearing capacity of the system in the SSW3C1F model has increased from about 3500 kN in the SSW3 model to approximately 6300 kN. In fact, it has increased by 80%. Also, the ductility coefficient in the case of using CFRP on the infill plate is equal to 7.35. This indicates an increase in shear capacity and energy dissipation, and a decrease in system ductility compared to the SSW3 model. Absorption energy in this model is about 2 times of the SSW3 model. Diagonal buckling is prevented if CFRP layer is used. Also, by a simple comparison between the maximum in-plane displacement between the SSW3 and SSW3C1F models, it can be clearly seen that, with the presence of CFRP, the out-of-plane displacement is reduced 10 times. This confirms the positive effect of CFRPs on the behavior of the system. In this model, with increasing load cycles, it is observed that CFRP sheets were able to absorb a lot of input energy and prevent premature buckling of the wall steel plate. Thus, it can be seen that the steel frame remains in the elastic zone, and only part of the plate wall has reached its yield stress.

By adding two layers of CFRP with a width of 50 cm and a length of 240 cm as a cross-coverage on one side of the steel infill plate, the load-bearing capacity of the frame has increased from about 3540 kN in the SSW3 model to 4100 kN. In fact, it has increased by 15.8%. Also, the ductility coefficient, in this case, is equal to 8.92. This indicates an increase in shear capacity and energy dissipation of the system. By adding two CFRP sheets on both sides of the steel plate between the HBEs and VBEs, the load-bearing capacity of the frame has increased from about 480 to 7000 kN. In fact, it has increased 13.6 times. Also, the ductility coefficient in the case of using a steel plate with a thickness of 3 mm is equal to 7.12. In this system, unlike previous models, no yield has occurred. The presence of two layers

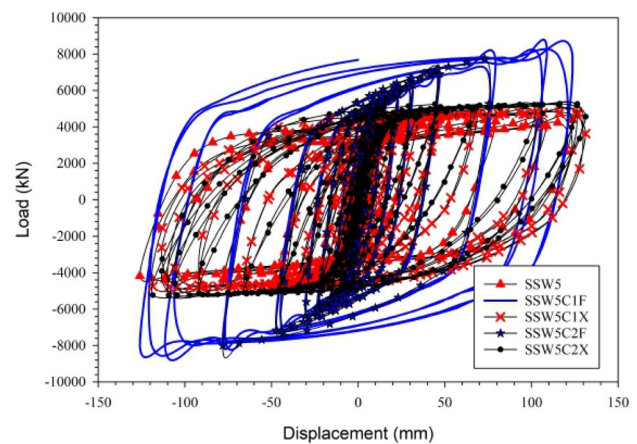


**Fig. 6** Comparison of force–displacement diagram of the frame with 5 mm thick SPSW

of CFRPs on both sides of the steel wall has improved and increased lateral load-bearing capacity, ductility, and energy dissipation.

## 5.2 Steel wall with a thickness of 5 mm

Figure 6 shows the hysteresis curve of a model set consisting of a steel sheet of 5 mm thickness. By adding only one steel plate between the boundary elements to a thickness of 5 mm, the load-bearing capacity of the frame has increased from about 480 to 4380 kN. In fact, it has increased by 900%. Also, a ductility coefficient of 8.25 has been obtained. Under lateral loading, the corner of the steel wall first yields at the junction of the beam to the column, and out of plane buckling in the direction of the tensile field occurred. Thus, by the end of the loading process, only the steel plate of the wall buckled and absorbed the input energy. Part of the column

flange in the area below the panel zone has also reached its yield stress. By adding only one layer of CFRP with a thickness of 0.176 mm to a steel plate with a thickness of 5 mm, the load-bearing capacity has reached 7960 kN. In fact, it has increased by 81.7% compared to the SSW5 model. Also, the ductility coefficient was obtained when using a layer of CFRP with a thickness of 0.176 mm, equal to 7.65. In this model, with increasing load cycles, it is observed that CFRP sheets were able to absorb a lot of input energy and prevent premature buckling of the wall steel plate. Thus, it can be seen that the steel frame remains in the elastic zone, and only part of the wall has reached its yield stress.

By CFRP sheet on one side of the wall steel plate, the load-bearing capacity of the frame has increased from about 4380 kN in the case of a frame with a 5 mm thick steel wall to 4840 kN in the SSW5C1X model. In fact, it has increased by 10.5%. Also, the ductility coefficient, in this case, is equal to 8.23.

By adding two CFRP sheets with full coverage of the infill wall, the load-bearing capacity of the frame has increased from about 480 kN in the MRF model to 8000 kN. In fact, it has increased 16 times. Also, the ductility coefficient in the mode of use is equal to 6.65. Figure 7 shows the out-of-plane deformation of the shear wall in the upper parts. When using CFRP sheets on both sides of the steel wall, most of the columns have yielded and have not reached the ultimate stress. This happens as the FRP layer reaches its final stress. No yielding or decrease in load-bearing capacity was observed. By changing the CFRP arrangement sheet from the whole wall state to cross-coverage, the load-bearing capacity of the frame has increased from about 4380 kN in the SSW5 model

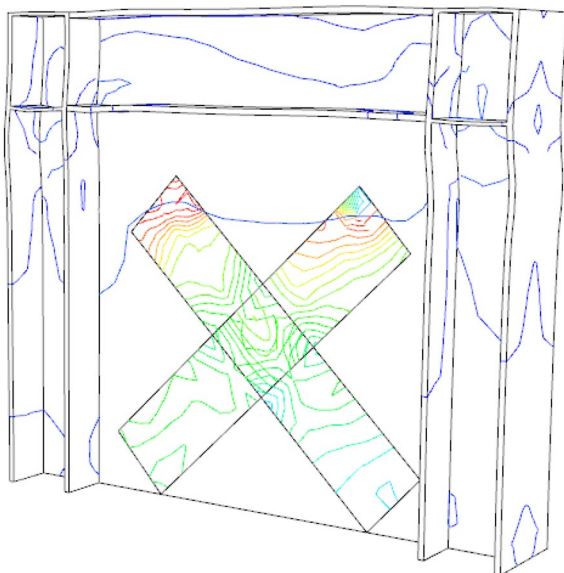


Fig. 7 Deformation in the direction perpendicular to the frame in the whole frame system and steel shear wall in the last step

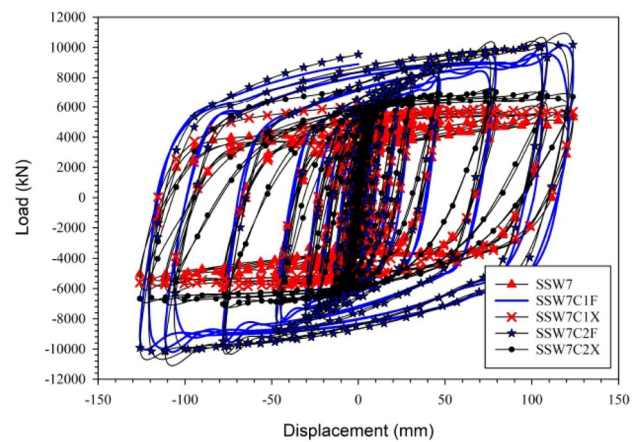


Fig. 8 Comparison of force–displacement diagram of the frame with 7 mm thick steel shear wall

to 5270 kN. In fact, it has increased by 20.3%. The ductility coefficient is also equal to 7.36.

### 5.3 Steel wall with a thickness of 7 mm

In this type of numerical models, a 7 mm thickness steel infill plate is added to the moment-resisting frame. Figure 8 shows the set of force–displacement behavior of the models. The load-bearing capacity of the frame has increased from about 480 to 5320 kN, which indicates a 10 times increase compared to the moment frame system. Also, the ductility coefficient is equal to 8.95. Figure 9 shows the stress distribution and deformation of the out-of-plane steel shear wall in the upper sections. In this case, even adding the thickness of the steel wall plate does not prevent the occurrence of out-of-plane buckling in the steel wall. This buckling is caused by the compressive load. In this case, even part of the

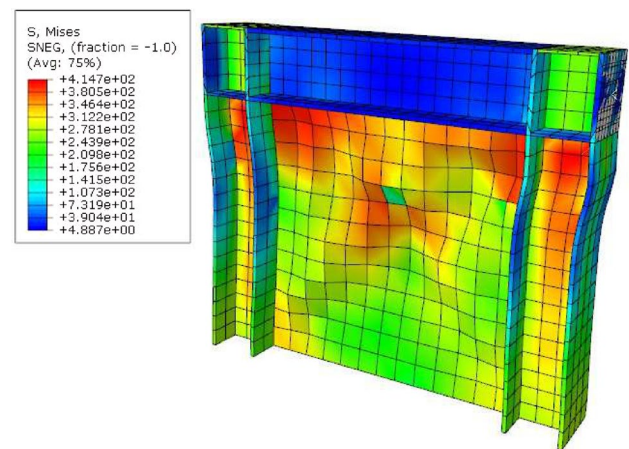


Fig. 9 Von Mises stress distribution throughout the frame system and steel shear wall

column head in the lower part of the panel zone has reached the yielding area.

Now, by adding a layer of CFRP sheet with a thickness of 0.176 mm with full coverage on one side of the steel plate, the load-bearing capacity of 9170 kN is obtained. In fact, it has increased by 72.4% compared to the SSW7 model. Also, the ductility coefficient was obtained when using a layer of CFRP with a thickness of 0.176 mm, equal to 7.73. By cross-coverage of the CFRP sheet on one side of the steel plate, the load-bearing capacity is approximately 6070 kN, which is an increase of approximately 14% compared to the SSW7 model. Also, the ductility coefficient, in this case, is equal to 7.46.

In the SSW7C2F model, the load-bearing capacity is approximately 1087 kN, and the ductility coefficient is calculated to be 7.34. The use of two layers of CFRP sheet on both sides of the steel wall increases the stiffness after the yielding of the curve. In other words, the stiffness drop is less than a model with a CFRP layer on one side. By cross-coverage of the FRP sheet on both sides of the steel plate, the load-bearing capacity increased by 35% compared to the SSW7 model, and the ductility coefficient was equal to 7.15.

## 5.4 Energy absorption

Energy absorption is one of the most important aspects of studying the seismic behavior of any structure. Ductile

**Table 2** Summary of the results of retrofitted and non-retrofitted models

Model name	Ductility	Ratio*	Maximum shear capacity (kN)	Percentage coverage** (%)
MRF	6.34	–	486.07	–
SSW3	9.14	1	3537.74	–
SSW3C1F	7.35	1.89	6710.06	50
SSW3C1X	8.92	1.16	4098.58	20.83
SSW3C2F	7.12	1.99	7025.60	100
SSW3C2X	8.85	1.26	4456.65	41.67
SSW5	8.25	1	4381.88	–
SSW5C1F	7.65	1.82	7959.71	50
SSW5C1X	8.23	1.1	4836.62	20.83
SSW5C2F	6.65	1.77	7748.63	100
SSW5C2X	7.36	1.2	5271.48	41.67
SSW7	8.95	1	5319.33	–
SSW7C1F	7.73	1.72	9169.13	50
SSW7C1X	7.46	1.14	6067.30	20.83
SSW7C2F	7.34	1.92	10,187.12	100
SSW7C2X	7.15	1.35	7193.96	41.67

\*The ratio of the capacity of the retrofitted model to the model without strengthening

\*\*Percentage of wall occupation area by carbon polymer fibers

behavior always takes precedence over rigid behavior, because the structure is able to withstand many deformations without failure. Energy dissipation during loading is equal to the area enclosed in each ring of the force–displacement hysteresis curve.

In Table 2, in the section of energy absorption ratio, it is mentioned that these numbers are measured by dividing the amount of energy absorption in each category of CSPSW with the same thickness compared to the sample without retrofitting in the same group. Also, the level of occupation in Table 2 means that both sides of the wall were considered as levels. Therefore, for a full polymer sheet on one side, the occupancy level will be 50%.

According to the results, it can be stated that by adding CFRP sheets to the steel wall in all models, the elastic stiffness and the shear capacity increased. As a result, the viscosity of the structure increases, which in turn improves the behavior of the structure. The highest capacity is related to the use of two layers of CFRP sheet in a steel wall with a thickness of 7 mm at a rate of approximately 10,187 kN, and the lowest value is related to the state of a steel wall with a thickness of 3 mm without strengthening at a rate of 3538 kN. Also, the effect of using one layer of CFRP sheet in increasing the load-bearing capacity is much more than the base model if using two layers of CFRP sheet. This means that using a layer of complete FRP sheet in the SPSW with a thickness of 3 mm, has been able to increase the lateral load-bearing capacity of the system by 89%. While adding another layer to the other side of the wall, the system capacity has increased by only 5% compared to when a surface is covered. By adding a layer of CFRP sheet to the other walls with a thickness of 5 and 7 mm, the load-bearing capacity increases by 10% and 11% compared to the use of a layer of CFRP sheet on one side.

By doubling the occupancy level of a steel shear wall, the load-bearing capacity follows the following equation. Of course, the following relationship is not completely general and can only be presented in this article. More comprehensive studies are needed to generalize this or other relationships.

$$F = -0.5733n^2 + 109.34n + 1866.8 \quad \text{for thickness 3 mm}$$

$$F = -0.5894n^2 + 124.32n + 2262 \quad \text{for thickness 5 mm}$$

$$F = -0.7254n^2 + 142.04n + 3268.6 \quad \text{for thickness 7 mm}$$

In the above equations, F represents the system capacity, and n represents the surface coverage ratio.

Interestingly, with the addition of CFRP sheets, the ductility of the structure is reduced compared to the non-retrofitted system. In other words, the behavior of the structure becomes more brittle in the presence of CFRPs. By



increasing the thickness of the steel wall and using CFRP sheets, the ductility is reduced compared to the models without a strengthening method. The ductility of the structure in the case of using CFRP s as a complete coating is less than in the case of cross-coverage. Using cross-coverage due to the level of occupation increases the load-bearing capacity to 40%. Comparing these two coverage modes, it seems that by comparing from an economic point of view, the x coverage mode could be more appropriate.

### 5.5 The effect of thickness increase on the behavior of FE models

The effect of the increase in the thickness of the infill plate on the cyclic behavior of the moment-resisting frame system is shown in Fig. 10. According to Fig. 10, increasing the thickness enhances the energy loss, initial stiffness and

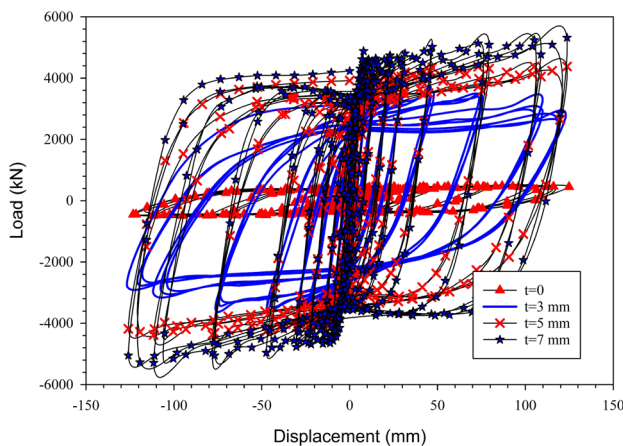


**Fig. 10** Comparison of force–displacement diagram of the frame with steel shear wall with different thicknesses

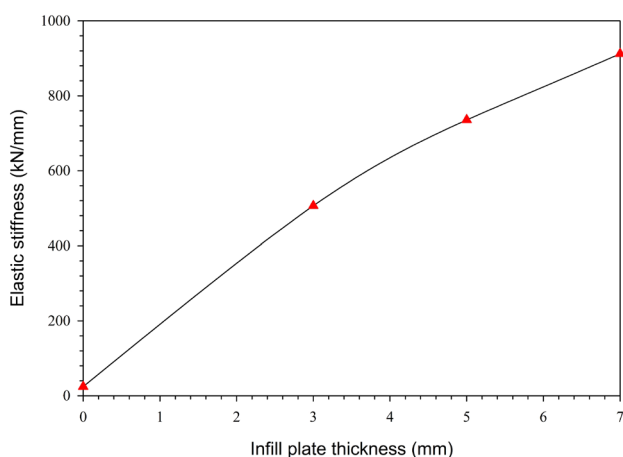


**Fig. 11** Relationship between shear wall steel sheet thickness and elastic stiffness

ultimate strength, and declines the decreasing rate of resistance in the pinching condition. Approximately by using 10 times of the plate thickness, the energy dissipation increases 10 times, but the connections of the beam to the column and the floor of the column must withstand the increase of the applied force. Because fracture connections are not considered in the model, the plate thickness can be increased to a certain extent. Figure 11 revealed that by increasing the plate thickness, the initial stiffness was elevated. As the thickness of the plate almost triples, the stiffness doubles.

A brief look at Fig. 11 shows that as the thickness of the steel plate increases, the initial stiffness of the system increases. This increase is partly linear and with a slope of 120 kN/mm. By adding FRP sheets with each arrangement, this slope varies from 50 to 200% growth. According to the shapes of the hysteresis curve of the models, it can be observed that there are hysteresis rings in the case without strengthening the model's degradation behavior or decreasing the resistance. In other words, in the non-retrofitted model, the stiffness is reduced. However, in the case of CFRP sheets, even with the lowest level of occupation of the steel wall, a decrease in strength or reduction in stiffness is observed. Also, adding CFRP sheets in two ways does not have a significant effect on the behavior of the structure and the hysteresis curve. Finally, increase the shear capacity by about 20%. Another point to note is that in all coating cases, the direction of the CFRP sheets in the diagonal direction (diagonal tensile field in the steel wall) with an angle of approximately 45 degrees, which has the greatest effect on the behavior of the structure. In the CFRP sheet with full coverage, the CFRPs are placed at an angle of approximately 45°, and in cross-coverage models, the CFRPs are placed at an angle of zero degrees. Because by turning the CFRP sheet in the direction of the infill plate diameter, the direction of CFRPs is in the same direction of the tensile field.

In the case of strengthening steel walls with CFRP sheets, the magnitude of accumulated energy dissipation inside the hysteresis rings is much higher than in the case without reinforcement. However, by adding CFRPs on two large sides, no significant effect was observed compared to strengthening on one side of the steel wall (maximum 25% increase in energy dissipation).

## 6 Conclusions

In this paper, the nonlinear behavior of a CSPSW system in which the steel wall is retrofitted by CFRP layers is investigated and analyzed in terms of FE models. Numerical models were planned to evaluate the effect of arrangement and type of coverage on steel wall occupation surface, steel wall thickness, and CFRP sheet thickness on stiffness,



shear strength, and other important seismic parameters. The important results of numerical analysis are as follows.

- If the steel infill plate among the moment-resisting frame is strengthened with CFRP sheets, the failure and ultimate strength of the composite system will increase significantly. Increasing the final strength of the system if using a 3 mm steel sheet is approximately 7.3 times that of the bending moment frame, and using a CFRP sheet on one side as a complete cover is about 2 times that of using a single steel plate. This amount of increase in thicker plates and using CFRP sheets on both sides of the wall is up to 15 times compared to the moment-resisting frame and nearly 3 times compared to the steel wall alone.
- The position of CFRPs in the direction of the tensile stress field of the steel wall is an important parameter in shear strength. In other words, by creating a tensile stress field, it prevents distortion and lateral buckling of the steel infill plate.
- If the SPSW is retrofitted with CFRP layers, the initial and secondary stiffnesses of the composite SPSW system will increase significantly. The purpose of increasing the secondary stiffness is to prevent a drop in shear resistance.
- Cumulative energy dissipation is much higher in retrofitted models than in non-retrofitted models. This value in the case of a steel wall with a thickness of 3 mm with a CFRP sheet on one side is approximately 2.5 times that of the model without reinforcement. In other models, this value varies between 1.5 and 4.0 times.
- Based on the research, the performance of SPSW with different types of FRP sheets should be studied. Also, another option for studying the behavior of the system can be unbonded SPSW to the vertical column to mitigate the over-size of column dimension.

**Funding** The authors have not disclosed any funding.

## Declarations

**Conflict of interest** The authors declare that they have no conflicts of interest.

## References

1. Rezaei M (1999) Seismic behaviour of steel plate shear walls by shake table testing. University of British Columbia. <https://doi.org/10.14288/1.0050150>
2. Driver RG, Kulak GL, Kennedy DL, Elwi AE (1998) Cyclic test of four-story steel plate shear wall. *J Struct Eng* 124(2):112–120. [https://doi.org/10.1061/\(ASCE\)0733-9445\(1998\)124:2\(112\)](https://doi.org/10.1061/(ASCE)0733-9445(1998)124:2(112))
3. Ashrafi HR, Beiranvand P, Pouraminian M, Moayeri MS (2018) Examining the impact of sheet placement and changes in waves characteristics on behavior of wavy steel shear wall. *Case Stud Constr Mater* 9:e00180. <https://doi.org/10.1016/j.cscm.2018.e00180>
4. Chen S-J, Jhang C (2006) Cyclic behavior of low yield point steel shear walls. *Thin-Walled Struct* 44(7):730–738. <https://doi.org/10.1016/j.tws.2006.08.002>
5. Chen S-J, Jhang C (2011) Experimental study of low-yield-point steel plate shear wall under in-plane load. *J Constr Steel Res* 67(6):977–985. <https://doi.org/10.1016/j.jcsr.2011.01.011>
6. Uy B, Bradford M (1996) Elastic local buckling of steel plates in composite steel-concrete members. *Eng Struct* 18(3):193–200. [https://doi.org/10.1016/0141-0296\(95\)00143-3](https://doi.org/10.1016/0141-0296(95)00143-3)
7. Kurata M, Leon R, DesRoches R, Nakashima M (2012) Steel plate shear wall with tension-bracing for seismic rehabilitation of steel frames. *J Constr Steel Res* 71:92–103. <https://doi.org/10.1016/j.jcsr.2011.10.026>
8. De Matteis G, Ahmadi HM (2021) Hysteretic behavior of steel shear panels with internal rectangular-shaped links. *J Constr Steel Res* 177:106451. <https://doi.org/10.1016/j.jcsr.2020.106451>
9. Thorburn LJ, Montgomery C, Kulak GL (1983) Analysis of steel plate shear walls. *Struct Eng Rep SER*. <https://doi.org/10.7939/R3BG2HB64>
10. Takahashi Y, Takeda T, Takemoto Y, Takagi M (1973) Experimental study on thin steel shear walls and particular steel bracing under alternative horizontal load. IABSE reports of the working commissions, 185–191. <https://doi.org/10.5169/seals-13766>
11. Alinia M, Dastfan M (2007) Cyclic behaviour, deformability and rigidity of stiffened steel shear panels. *J Constr Steel Res* 63(4):554–563. <https://doi.org/10.1016/j.jcsr.2006.06.005>
12. Alinia M, Shirazi RS (2009) On the design of stiffeners in steel plate shear walls. *J Constr Steel Res* 65(10–11):2069–2077. <https://doi.org/10.1016/j.jcsr.2009.06.009>
13. Habashi H, Alinia M (2010) Characteristics of the wall–frame interaction in steel plate shear walls. *J Constr Steel Res* 66(2):150–158. <https://doi.org/10.1016/j.jcsr.2009.09.004>
14. Deng E-F, Zong L, Ding Y (2019) Numerical and analytical study on initial stiffness of corrugated steel plate shear walls in modular construction. *Steel Compos Struct* 32(3):347–359. <https://doi.org/10.12989/scs.2019.32.3.347>
15. Luo Q, Wang W, Sun Z, Xu S, Wang B (2021) Seismic performance analysis of corrugated-steel-plate composite shear wall based on corner failure. *J Constr Steel Res* 180:106606. <https://doi.org/10.1016/j.jcsr.2021.106606>
16. Wang W, Luo Q, Sun Z, Wang B, Xu S (2021) Relation analysis between out-of-plane and in-plane failure of corrugated steel plate shear wall. *Structures* 29:1522–1536. <https://doi.org/10.1016/j.istruc.2020.12.030>
17. Astaneh-Asl A (2000) Seismic studies of innovative and traditional composite shear walls. Research project in-progress. Univ. of California, Berkeley: Dept. of Civil and Env. Engineering
18. Arabzade A, Moharami H, Ayazi A (2011) Local elastic buckling coefficients of steel plates in composite steel plate shear walls. *Scientia Iranica* 18(1):9–15. <https://doi.org/10.1016/j.scient.2011.03.002>
19. Dan D (2012) Experimental tests on seismically damaged composite steel concrete walls retrofitted with CFRP composites. *Eng Struct* 45:338–348. <https://doi.org/10.1016/j.engstruct.2012.06.037>
20. Ali MM, Osman S, Husam O, Al-Zand AW (2018) Numerical study of the cyclic behavior of steel plate shear wall systems

- (SPSWs) with differently shaped openings. *Steel Compos Struct* 26(3):361–373. <https://doi.org/10.12989/scs.2018.26.3.361>
21. Massumi A, Karimi N, Ahmadi M (2018) Effects of openings geometry and relative area on seismic performance of steel shear walls. *Steel Compos Struct* 28(5):617–628. <https://doi.org/10.12989/scs.2018.28.5.617>
  22. Zhang X, Ren Q, Wang J, Liu Z, Yang X (2021) Numerical simulation and shear capacity study of a new double-steel-plate shear wall. *Adv Civ Eng* 2021:14. <https://doi.org/10.1155/2021/5925369> (Article ID 5925369)
  23. Li Y, Zhao X, Tan P, Zhou F, Jiang J (2021) Seismic behavior of a novel buckling-restrained steel plate shear wall. *Shock Vib* 22:1–21. <https://doi.org/10.1155/2021/5599578>
  24. Hatami F, Ghamari A, Rahai A (2012) Investigating the properties of steel shear walls reinforced with carbon fiber polymers (CFRP). *J Constr Steel Res* 70:36–42. <https://doi.org/10.1016/j.jcsr.2011.07.010>
  25. Nateghi-Alahi F, Khazaei-Poul M (2012) Experimental study of steel plate shear walls with infill plates strengthened by GFRP laminates. *J Constr Steel Res* 78:159–172. <https://doi.org/10.1016/j.jcsr.2012.07.002>
  26. Dan D, Fabian A, Stoian V (2011) Theoretical and experimental study on composite steel–concrete shear walls with vertical steel encased profiles. *J Constr Steel Res* 67(5):800–813. <https://doi.org/10.1016/j.jcsr.2010.12.013>
  27. Seddighi M, Barkhordari MA, Hosseinzadeh S (2019) Behavior of FRP-reinforced steel plate shear walls with various reinforcement designs. *Steel Compos Struct* 33(5):729–746. <https://doi.org/10.12989/scs.2019.33.5.729>
  28. ABAQUS, User's Manual (2016) Dassault systemes simulia corporation, Providence
  29. Ebadi Jamkhaneh M, Kafi MA, Kheyroddin A (2019) Behavior of partially encased composite members under various load conditions: experimental and analytical models. *Adv Struct Eng* 22(1):94–111. <https://doi.org/10.1177/1369433218778725>
  30. Jamkhaneh ME, Ahmadi M, Sadeghian P (2020) Simplified relations for confinement factors of partially and highly confined areas of concrete in partially encased composite columns. *Eng Struct* 208:110303. <https://doi.org/10.1016/j.engstruct.2020.110303>
  31. Ebrahimi AH, Ebadi Jamkhaneh M, Shokri Amiri M (2018) 3D finite-element analysis of steel moment frames including long-span entrance by strengthening steel cables and diagonal concentrically braced frames under progressive collapse. *Pract Period Struct Des Constr* 23(4):04018025. [https://doi.org/10.1061/\(ASCE\)SC.1943-5576.0000388](https://doi.org/10.1061/(ASCE)SC.1943-5576.0000388)

**Publisher's Note** Springer Nature remains neutral with regard to jurisdictional claims in published maps and institutional affiliations.